

A Unified Approach to Global and Local Beam Position Feedback*

Y. Chung

Argonne National Laboratory, Argonne, IL 60439, U.S.A.

Abstract

The Advanced Photon Source (APS) will implement both global and local beam position feedback systems to stabilize the particle and X-ray beams for the storage ring. The global feedback system uses 40 BPMs and 40 correctors per plane. Singular value decomposition (SVD) of the response matrix is used for closed orbit correction. The local feedback system uses two X-ray BPMs, two rf BPMs, and the four-magnet local bump to control the angle and displacement of the X-ray beam from a bending magnet or an insertion device. Both the global and local feedback systems are based on digital signal processing (DSP) running at 4-kHz sampling rate with a proportional, integral, and derivative (PID) control algorithm. In this paper, we will discuss resolution of the conflict among multiple local feedback systems due to local bump closure error and decoupling of the global and local feedback systems to maximize correction efficiency. In this scheme, the global feedback system absorbs the local bump closure error and the local feedback systems compensate for the effect of global feedback on the local beamlines. The required data sharing between the global and local feedback systems is done through the fiber-optically networked reflective memory.

1. INTRODUCTION

The Advanced Photon Source (APS) is one of the third-generation synchrotron light sources which are characterized by low emittance of the charged particle beams and high brightness of the photon beams radiated from insertion devices. In order to achieve the stringent transverse X-ray beam position stability required by the current user community, we are developing an extensive beam position feedback systems with the correction bandwidth approaching 100 Hz. [1-3]

The APS storage ring has 360 rf beam position monitors (BPMs) and 318 corrector magnets distributed around the storage ring, miniature BPMs for insertion device beamlines, and photon beam position monitors in the front end of X-ray beamlines for global and local orbit correction. The real-time (AC) feedback systems, which are the main focus of this work, will use a subset of these to counteract the effect of various vibration sources, including the ground vibration, mechanical vibration of the accelerator subcomponents, thermal effect, and so forth.

The feedback systems can be largely divided into the global and local feedback systems according to the scope of correction. The global feedback system uses 40 rf BPMs and 40 corrector magnets distributed equally in 40 sectors. The

primary function is to stabilize the selected perturbation modes of the global orbit. The local feedback systems, on the other hand, stabilize the source regions of the X-ray beams locally for angle and displacement.

An ideal local feedback system would not affect the rest of the closed orbit including other local feedback systems. In reality, the global and local feedback systems constantly interact with one another. The effect of global orbit feedback unavoidably interferes with the local feedback. On the other hand, the bump closure error in the local feedback due to bump coefficient error, magnet field error, eddy current effect, etc., causes global orbit perturbation and affects other local feedback systems. If this interaction is too strong, the feedback systems can become ineffective, oscillatory, or even unstable. In order to minimize such effects and maximize the feedback efficiency, it is necessary to decouple the global and local feedback systems. The local feedback compensates for the effect of the global feedback and the global feedback reduces the effect of local bump closure error.

In this work, we will investigate the effect of coupling among global and multiple local feedback systems and how to resolve it through decoupling. The remainder of this paper will be a theoretical review of the dynamics of global and local feedback systems in Section 2, and analysis of the APS feedback systems in Section 3.

2. THEORY

2.1 Feedback System Description

Let us consider a feedback system comprised of global and non-overlapping local feedback systems. In the following discussion, the subscripts g and l denote global and local feedback, respectively, unless noted otherwise.

The global feedback uses M BPMs to obtain the orbit and N correctors to reduce perturbation. The global response matrix \mathbf{R}_g defined as the beam motion at BPM locations per unit kick by corrector magnets, is then an $M \times N$ matrix.

In case the local feedback system controls both the angle and displacement of the photon beam, at least two monitors and four correctors are necessary per beamline. In this case the local bump can be decomposed into two independent three-magnet local bumps a and b as shown in Fig. 1. The angle and position of the photon beam can be controlled by adjusting strengths of the a and b bumps. Traditionally two X-ray BPMs are used to measure the photon beam positions, but two rf BPMs inside the local bump may also be used. We further assume that the none of the BPMs used by the local feedback systems is used by the global feedback. In any case, the local response matrix \mathbf{R}_l can be reduced to a 2×2 matrix

*Work supported by the U.S. Department of Energy, Office of Basic Energy Sciences, under Contract No. W-31-109-ENG-38.

relating the angle and displacement of the photon beam and the two bump strengths.

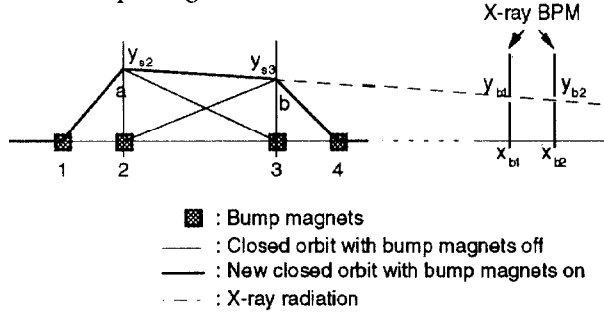


Fig. 1: Schematic of the local feedback system.

2.2 Inversion of the Response Matrix

The response matrix \mathbf{R} combines the global response matrix \mathbf{R}_g , collective response matrices \mathbf{R}_l for L local feedback systems, the global-to-local response matrix \mathbf{R}_{lg} , and the local-to-global response matrix \mathbf{R}_{gl} as shown in Fig. 2. \mathbf{R}_{lg} represents the effect of global correctors on the local beam positions, and \mathbf{R}_{gl} represents the effect of local bump closure error on the global orbit. The shaded area of \mathbf{R} in Fig. 3 is due to the local bump closure error.

The inverse response matrix \mathbf{R}_{inv} is the matrix used to obtain the corrector strength vector $\Delta\theta$ to correct the orbit error Δy , that is,

$$\Delta\theta = \mathbf{R}_{inv} \cdot \Delta y. \quad (1)$$

Like the response matrix \mathbf{R} , the inverse response matrix \mathbf{R}_{inv} is a composition of three component matrices, \mathbf{R}_{ginv} , \mathbf{R}_{linv} and $\mathbf{R}_{inv,lg}$ as shown in Fig. 2. In this work, the global inverse matrix \mathbf{R}_{ginv} was obtained using the singular value decomposition (SVD) of the response matrix.[1,2,5,6] The details of the SVD technique can be found in the references and will not be discussed in this paper. The local inverse matrix \mathbf{R}_{linv} is obtained by inverting the 2×2 local response matrices.

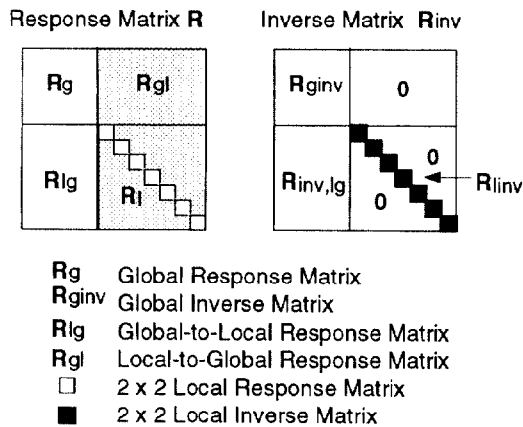


Fig. 2: Response matrix and its inverse for the unified feedback system.

The remaining component matrix $\mathbf{R}_{inv,lg}$ is determined such that the effect of the global correctors on the local feedback is canceled by considering the global and local feedback systems as a single, unified feedback system. This can be done by setting

$$\mathbf{R}_{inv,lg} = -\mathbf{R}_{linv} \cdot \mathbf{R}_{lg} \cdot \mathbf{R}_{ginv}. \quad (2)$$

The physical interpretation of Eq. (2) can be given as follows. \mathbf{R}_{ginv} is the response of the global correctors to global orbit perturbation, \mathbf{R}_{lg} is the local orbit perturbation due to global correctors, and \mathbf{R}_{linv} is the response of the local correctors to local orbit perturbation. The matrix product $\mathbf{R}_{linv} \cdot \mathbf{R}_{lg} \cdot \mathbf{R}_{ginv}$ is then the response of the local correctors to global orbit perturbation and $\mathbf{R}_{inv,lg}$ in Eq. (2) compensates for the action of the global feedback on the local orbits, resulting in maximum orbit correction efficiency.

2.3 Feedback System Dynamics

The schematic diagram of the feedback system is shown in Fig. 3. We assume a digital feedback system and will analyze it using the technique of Z-transform.[4] The sampling time is T and the sampling frequency F_s is equal to $1/T$. $\{s_n\}$ and $\{y_n\}$ are the discrete sequences of vectors representing the reference and measured orbits. The gain matrix \mathbf{G} includes the feedback controller and a bandwidth-limiting filter, and the matrix \mathbf{H} represents the BPM bandwidth. The external perturbation is given by $\{w_n\}$.

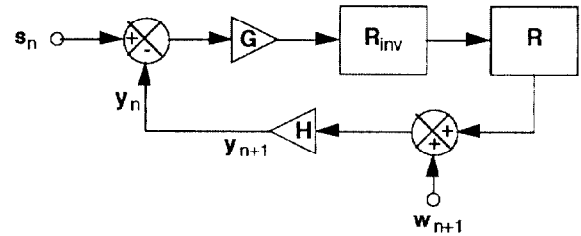


Fig. 3: The schematic diagram for the global beam position feedback system.

The difference equation describing the response of the feedback system in Fig. 3 is given by

$$y_{n+1} = \mathbf{H} \cdot \{ \mathbf{R} \cdot \mathbf{R}_{inv} \cdot \mathbf{G} \cdot (s_n - y_n) + w_{n+1} \}. \quad (3)$$

Applying the Z-transform to Eq. (3), we obtain

$$\mathbf{Y}(z) = \left\{ \mathbf{1} - \mathbf{F}(z) \frac{\mathbf{1}}{\mathbf{H}(z)} \right\} \cdot \mathbf{S}(z) + \mathbf{F}(z) \cdot \mathbf{W}(z) \quad (4)$$

where

$$\mathbf{F}(z) = \frac{\mathbf{1}}{\mathbf{1} + \mathbf{H}(z) \cdot \mathbf{R} \cdot \mathbf{R}_{inv} \cdot \mathbf{G}(z) z^{-1}} \mathbf{H}(z). \quad (5)$$

$\mathbf{Y}(z)$ is the Z-transform of $\{y_n\}$, $\mathbf{W}(z)$ is the Z-transform of $\{w_n\}$ and so forth. The expression $1/(\cdot)$ denotes the inverse matrix. The matrix $\mathbf{F}(z)$ is the noise-filter matrix and with the substitution $z = \exp(-i\omega T)$, we can obtain the frequency

response of the feedback system. The last term in Eq. (4) represents the residue of the perturbation in the orbit with feedback.

Using Eq. (2) and assuming $\mathbf{R} \cdot \mathbf{R}_{\text{inv}} = \mathbf{1}$, it can be shown that the matrix product $\mathbf{R} \cdot \mathbf{R}_{\text{inv}}$ is given by

$$\mathbf{R} \cdot \mathbf{R}_{\text{inv}} = \mathbf{R}_g \cdot \mathbf{R}_{g\text{inv}} \oplus \mathbf{1}_1 \quad (6)$$

in the ideal case of no local bump closure error. The operator \oplus combines two matrices as depicted in Fig. 4.

$$\begin{bmatrix} \mathbf{X} \end{bmatrix} \oplus \begin{bmatrix} \mathbf{Y} \end{bmatrix} = \begin{bmatrix} \mathbf{X} & \mathbf{0} \\ \mathbf{0} & \mathbf{Y} \end{bmatrix}$$

Fig. 4: The matrix combination operator \oplus .

Now, putting

$$\mathbf{G}(z) = G_g(z) \mathbf{1}_g \oplus G_l(z) \mathbf{1}_l \quad \text{and} \quad \mathbf{H}(z) = H_g(z) \mathbf{1}_g \oplus H_l(z) \mathbf{1}_l \quad (7)$$

we obtain

$$\mathbf{F}(z) = \mathbf{U} \cdot \mathbf{F}_g(z) \cdot \mathbf{U}^T \oplus \mathbf{F}_l(z), \quad (8)$$

where \mathbf{U} is the unitary global BPM transform matrix derived from SVD, and $\mathbf{F}_g(z)$ and $\mathbf{F}_l(z)$ are diagonal. Equation (8) indicates that there exists a coordinate transformation that decouples the feedback channels, and single-channel feedback theory can be applied to each channel.

Using the relation $\mathbf{U} \cdot \mathbf{U}^T = \mathbf{U}^T \cdot \mathbf{U} = \mathbf{1}$, we obtain from Eqs. (4) and (5) the diagonal elements of $\mathbf{F}_g(z)$ as

$$F_{g,ii}(z) = \begin{cases} \frac{H_g(z)}{1 + H_g(z)G_g(z)z^{-1}} & \text{coupled modes} \\ 0 & \text{decoupled modes} \end{cases} \quad (9)$$

and similarly for $\mathbf{F}_l(z)$. The noise filter matrix for the BPMs can be obtained from Eqs. (8) and (9). The expression for the coupled modes is identical to that of a single-channel feedback system.[3] The PID controller function $G(z)$ is given by

$$G(z) = K_P + \frac{K_I}{1 - z^{-1}} + K_D(1 - z^{-1}), \quad (10)$$

where K_P , K_I , and K_D are the proportional, integral, and derivative controller gains, respectively. When K_I is finite, the open loop DC gain is infinite, and therefore, the long-term drift can be completely corrected.

3. ANALYSIS OF THE APS FEEDBACK SYSTEM

In this section, we will discuss the results of simulation on the APS beam position feedback system with 20 local feedback systems. Due to the relatively thick (1/2") aluminum vacuum chamber at the location of local corrector magnets, a strong eddy current is induced in the vacuum chamber. This causes attenuation and phase delay of the applied magnetic field and generates a strong quadrupole magnetic field (13% per cm at 20Hz) inside the chamber. This leads to local bump

closure error when the particle beam is at a significant distance from the vacuum chamber center. The magnet field error due to calibration error and saturation adds to this effect.

Figure 5 shows simulated results comparing the cases when the global and local feedback systems are coupled ($\mathbf{R}_{\text{inv} \cdot \text{lg}} = \mathbf{0}$) and decoupled ($\mathbf{R}_{\text{inv} \cdot \text{lg}} = -\mathbf{R}_{\text{inv} \cdot \text{lg}} \cdot \mathbf{R}_{\text{lg}} \cdot \mathbf{R}_{g\text{inv}}$). It also shows the attenuation of noise by the feedback system. Random field error less than 2% and orbit deviation less than 3 mm were assumed with the vacuum chamber eddy current taken into account. The correction efficiency is shown in terms of the local corrector load (mrad/mm) necessary to correct a given orbit perturbation of global SVD eigenmodes. Decoupling the global and local feedback systems results in significant improvement in the correction efficiency beyond 10 Hz.

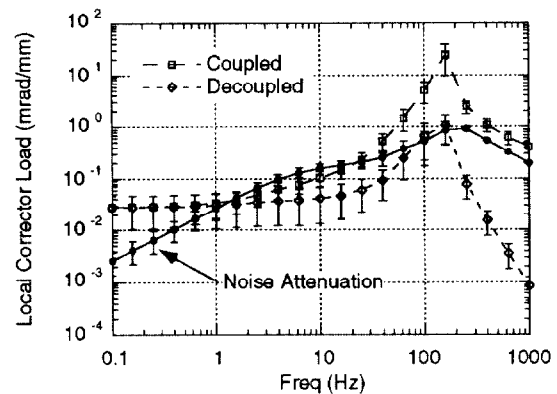


Fig. 5: Improvement of local orbit correction efficiency for the decoupled feedback system in correcting global SVD eigenmodes. Random field error less than 2% and orbit deviation less than 3 mm were assumed with the vacuum chamber eddy current taken into account.

5. REFERENCES

- [1] Y. Chung, G. Decker and K. Evans, Jr., "Closed Orbit Correction Using Singular Value Decomposition of the Response Matrix," *Proceedings of the 1993 IEEE Particle Accelerator Conference*, Washington, D.C., p. 2263, 1993.
- [2] Y. Chung, et al., "Global DC Closed Orbit Correction Experiments on the NSLS X-ray Ring and SPEAR," *Proceedings of the 1993 IEEE Particle Accelerator Conference*, Washington, D.C., p. 2275, 1993.
- [3] Y. Chung, L. Emery, and K. Kirchman, "Compensation for the Effect of Vacuum Chamber Eddy Current by Digital Signal Processing for Closed Orbit Feedback," *Proceedings of the 1993 IEEE Particle Accelerator Conference*, Washington, D.C., p. 2266, 1993.
- [4] A. Peled and B. Liu, *Digital Signal Processing*, John Wiley & Sons, 1976.
- [5] G. H. Golub and C. Reinsch, "Singular Value Decomposition and Least Squares Solutions," *Numer. Math.* **14**, pp. 403-420, 1970, and references therein. Also in J. H. Wilkinson and C. Reinsch, *Linear Algebra*, vol. II of *Handbook for Automatic Computation*, Springer-Verlag, New York, 1971.
- [6] K. J. Kleman, "Beam Diagnostics and Control at Aladdin," *Nuclear Inst. and Meth.*, **A266**, p. 172, 1988.